U.P.B. Sci. Bull., Series D, Vol. 74, Iss. 3, 2012 ISSN 1454-2358

A BUMPLESS TRANSFER METHOD FOR AUTOMATIC FLIGHT CONTROL SWITCHING

Andrei-Sorin NEAMTU[1], Adrian-Mihail STOICA[2]

Tehnicile de Control Adaptiv cu Supervizor si Comutație s-au stabilit în ultimele doua decenii ca o alternativă viabila de realizarea a controlului zborului adaptiv spre deosebire de alternativa pseudo-adaptiva oferita de programarea amplificărilor (gain-scheduling). Dar, oricât de promițătoare se dovedesc rezultatele oferite de aceste metode ele sunt de multe ori degradate de apariția unor creşteri bruşte ale semnalului la momentul comutării intre doua compensatoare. In aceasta lucrare autorii vor prezenta o metodă simpla de reducere a acestor creşteri şi realizării unui control eficient al aeronavei.

Adaptive Supervisory Switching Control techniques have emerged during the last two decades as a viable way of achieving true adaptive flight control as opposed to the pseudo-adaptive behavior offered by gain-scheduled flight controllers. However, the promising results offered by these methods are sometimes hampered by spikes appearing at the moment of switching from one controller to a new one. In this paper, the authors present a simple method to reduce these spikes and to provide a smooth control of the aircraft.

1. Introduction

Designing automatic flight control systems for high performance aircraft is a difficult and complex task. Due to the varied conditions in which such an aircraft must operate, a single control law obtained by conventional techniques is insufficient to be utilized over the whole envelope inside which the aircraft is supposed to operate. This is one of the reasons which lead to the issuing of requirements for adaptive flight control 50 years ago. Though a lot has been written on this issue, not many practical systems of this type have been implemented. The only active control system resembling adaptive control is the one based on the so called "gain scheduling" method. In this control scheme, a set of measurements from outside the system is used to identify the flight conditions in which the aircraft is operating and then a suitable control gain is selected corresponding to these conditions. However, this scheme has some drawbacks.

[1]Eng. National Institute for Aerospace Research „Elei Carafoli", PhD Student, University POLITEHINICA Bucharest, Faculty of Aerospace Engineering, e-mail: andreis.neamtu@gmail.com
[2] Prof. University POLITEHNICA of Bucharest, Faculty of Aerospace Engineering, Romania

The main one is that the measurements used to identify the flight conditions are taken from outside of the control loop which means that there is no guarantee that they will correctly represent the current conditions. It also means that there is no protection for the case in which the measurements are not accurate. Another drawback is that gain scheduling is used only for relatively low angles-of-attack, usually below 15 degrees, as the measurements normally used, indicating air speed and altitude taken with a Pitot tube, cannot be obtained correctly at angles of attack above 15 degrees.

These disadvantages of gain scheduling can be diminished by the use of Adaptive Switching Supervisory Control (ASSC) (see [1], [2], [3], and [4]). ASSC is in fact an adaptive version of classical gain scheduling, turned, by the use of a supervisory logic based on plant input/output recorded data, from an open loop switching mechanism to a closed loop one. A typical ASSC is depicted in Figure 1. A data driven "high-level unit" *S*, called *supervisor*, controls each plant G belonging to the given set $\mathcal{G}$ of plant models by connecting an appropriate controller *K* from the set $\mathcal{K}$ of candidate controllers The supervisor decides if the currently switched-on controller works properly, and, in the negative case, it replaces it by another candidate controller. The scheduling task (when to substitute the acting controller) and the routing task (which controller to switch on) are carried out in real time by monitoring purely data-driven test functional [1]. There are two distinct groups of ASSC methods, the first one consists in the so called *Multi-Model* ASSC (MASSC), wherein a dynamic nominal model is associated with every candidate controller; the second one, called *Unfalsified* ASSC (UASSC) ([1], [2]) uses a switching logic that dispenses with the need for a-priori knowledge of the used dynamic model of the controlled plant. Both these methods have their advantages and disadvantages. MASSC schemes work by comparing norms of sequences of estimation errors based on the various nominal models, as the candidate controller associated to the nominal model yielding the prediction norm of minimum magnitude is believed to be the most suitable one. The main advantage is the fact that transient time before finding a stabilizing controller is small. However this can be achieved only by using a very dense model distribution. If this condition is not imposed, neither convergence to a final controller, nor boundness can be guaranteed. In contrast, UASSC schemes as described by [2], can select in finite time a final controller with an optimum performance in reference to some previously selected *performance specification*, under the minimum conceivable requirement regarding the existence of a stabilizing candidate controller. This, along with the fact that the plant need not be linear, makes these schemes much better suited to aerospace applications then MASSC, from the robustness point of view the asymptotic stability properties of the latter being typically only guaranteed if the unknown plant is tightly approximated by at least one nominal model. However, the main disadvantage of

UASSC schemes used so far, as noted in [1] and [2], stems from the fact that they do not provide protection against the temporary insertion in the loop of destabilizing controllers, which might lead to long transient times and temporary trends to divergence before the final stabilizing controller is switched on. In the examples provided in [4] the supervisor needs about 70 seconds before finding the stabilizing controller, which would not be convenient when trying to stabilize the short period longitudinal dynamics of an aircraft.

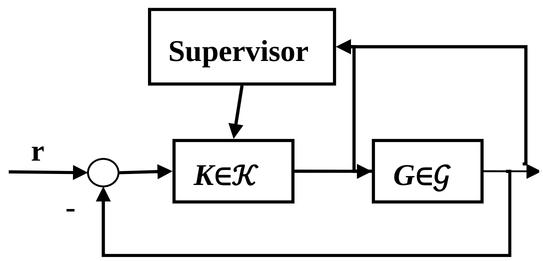

Fig 1 Adaptive Supervisory Switching Control scheme

For this reasons in [1] a scheme called Multi Model Unfalsified Adaptive Switching Supervisory Control, that combines the advantages of both methods (low transient times for MASSC and asymptotic stability for UASSC), was proposed.

For both adaptive methods briefly described above there is however a major disadvantage. At the instant when the old control law is discarded and a new one switched in its stead, sometimes the output of the plant can increase rapidly and then drop, generating what is called a bump. Mitigation this behavior has been a part of research on Switching Control since the 1980 and several methods are presented in papers such as [5], where a general anti-windup method is adapted for bumpless switching, [6], where a method which works without detailed knowledge of the plant is presented and [7] where a method specifically designed for Unfalsified ASSC is presented.

In this paper we shall integrate a simple bumpless transfer algorithm with Unfalsified ASSC. Unlike the algorithm presented in [7] we shall deal with the specific case of a highly maneuverable aircraft modeled using the benchmark ADMIRE model. Because of tailoring the application for aerospace control, where spikes in the control signal are a normal occurrence especially in air-combat scenarios, the main goal we are trying to achieve is a reduction in the bumps that ensures that the actuators do not saturate. Details regarding the synthesis of the adaptive switching Automatic Flight Control System can be found in [8] and [9]. In the current paper we will focus on the bumpless transfer aspects occurring when such adaptive control systems are used.

The paper is organized as follows: in the next section a brief description of the adaptive flight control system is given. The main idea of the bumpless transfer method is presented in Section 3.The proposed method is illustrated by a numerical case study in Section 4. The Paper ends with some concluding remarks and further developments in Section 5.

2. Adaptive automatic flight control system using unfalsified control techniques

In this section some basic ideas concerning the unfalsified adaptive control method will be briefly recalled. More details can be found for instance in [1] and [4] but here we focus our attention on the aspects directly required for aviation applications.

Consider the following closed loop control system:

$$\begin{aligned} y(s) &= G(s)u(s) \\ u(s) &= K(s)\big(r(s)-y(s)\big) \end{aligned} \tag{1}$$

where $G(s)$ denotes the transfer function of the controlled plant, $K(s)$ stands for the controller, r is the reference signal, u and y are the control variable and the system output respectively. Though UASSC methods can be used on non-linear plants, linearity will be assumed throughout the paper for simplicity (for more details see [8] and [9])

It is assumed that G belongs to a plant uncertainty set $\mathcal{G}$, while the controller K belongs to a finite family $\mathcal{K}$ of *Linear Time Invariant* (LTI) controllers.

Definition 1 *Given a signal x(t), t≥0 it is said that*

$$x_\tau(t) = \begin{cases} x(t),\ t\in[0,\tau] \\ 0,\ \textit{otherwise} \end{cases}$$

represents a truncation of x(t) with the truncated norm

$$\|x\|_\tau = \left(\int_0^\tau x^2(t)\,dt\right)^{\frac{1}{2}}.$$

With the above definition the following slight generalization of input-output stability will be adopted throughout the paper ([1], [2], [4]).

Definition 2 *A dynamic system with the input r and the output y is called stable, or the stability is unfalsified by the data* (*u, y*)*, if there exist α, β≥0 such that:*

$$\|y\|_\tau \le \alpha\|r\|_\tau + \beta\,,$$

∀ $\tau \geq 0$ and for all $r \in L_{2e}$, L_{2e} denoting the space of all functions with finite energy on any finite interval. Otherwise if $\sup_{\tau \geq 0 \|r\|_\tau \neq 0} \frac{\|y\|_\tau}{\|r\|_\tau} \to \infty$, *it is said that the stability of the system is falsified by the data* (u, y).

The presence of the term $\beta \geq 0$ in the above definition is related to the situation where non-zero initial conditions, of the system, are taken into account. The next definition will be used in the following developments (see also [1], [4]).

Definition 3 *The adaptive control problem is feasible if, for every* $G \in \mathcal{G}$, *there exists at least one controller* $K \in \mathcal{K}$ *such that the resulting system obtained by coupling K to G is stable and it accomplishes the performance objectives.*

The unfalsified adaptive control techniques are essentially based on the so-called *fictitious reference signal* and on an associated *performance index* which allows choosing appropriate controllers, $K \in \mathcal{K}$, for which the problem is feasible [4]

Definition 4 *Let the data* (u, y) *be the input and output measurements of a plant G over the time interval* $[0, \tau]$. *Then the fictitious reference signal* $\tilde{r}_K$ *associated to a controller* $K \in \mathcal{K}$ *is the signal defined over* $[0, \tau]$ *that produces the same set of data* (u, y) *if K would be connected to G.*

Note that the above definition requires the *invertibility* of *K* in which case the fictitious reference signal is given by $\tilde{r}_K = K^{-1}u + y$. This expression of $\tilde{r}_K$ reveals another major constraint for *K,* namely it must be *minimum phase* since otherwise the fictitious reference $\tilde{r}_K$ can be unbounded for $t \to \infty$. Some aspects concerning these constraints are discussed in more detail in [8] and [9].

The performance index $J(K, u, y, \tau)$ is a positive function defined on $\mathcal{K} \times \mathcal{U} \times \mathcal{Y} \times \mathbb{R}_+$ where *u* and *y* are truncated on the interval $[0, \tau]$. It is chosen according to the design specifications of the controller *K* and it represents a measure of the performance provided by *K* on the time interval $[0, \tau]$.

Definition 5 *A controller* $K \in \mathcal{K}$ *is called falsified at the time* τ *with respect to a given cost level* $\gamma > 0$ *by the data* (u, y) *measured on the time interval* $[0, \tau]$ *if* $J(K, u, y, \tau) > \gamma$. *Otherwise the controller K is called unfalsified by the measurements* (u, y) *on* $[0, \tau]$.

According to the terminology used in [4] the set of all unfalsified controllers with the unfalsified cost level $\gamma>0$ at time t stands for the *unfalsified controller set.*

> ***Definition 6*** *Consider the reference signal r and the measured set of data* (u, y) *obtained by a finite number of switches of controllers* $K\in\mathcal{K}$*, mapping* $\begin{bmatrix} r(t) \\ y(t) \end{bmatrix}$ *to* $u(t)$ *and denote by* t_f *the final switching time and by* K_f *the final controller. Then the pair* $(J,\mathcal{K})$ *is called cost-detectable if the following assertions are equivalent:*
>
> *a)* $J(K_f, u, y, \tau)$ *is monotonically increasing and bounded for* $\tau\to\infty$*;*
>
> *b) The closed loop system in Fig. 1 with* K_f *is unfalsified by the data* (u, y) *when* $\tau\to\infty$.

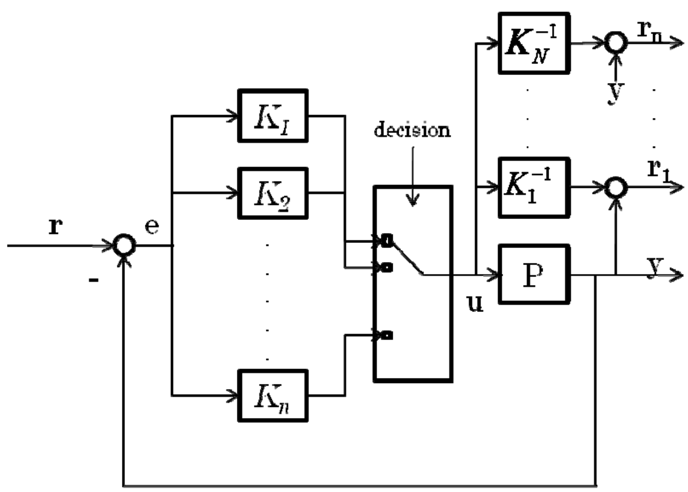

Fig. 2 Unfalsified Adaptive Supervisory Switching Control Scheme

A common performance index considered in the unfalsified control literature (see [2], [4], [10] for example) is:

$$J\left(K,u,y,\tau\right)=\frac{\left\|w_1*(y-\tilde{r})\right\|^2_{L_2[0,t]}+\left\|w_2*u\right\|^2_{L_2[0,t]}}{\left\|\tilde{r}\right\|^2_{L_2[0,t]}} \tag{2}$$

where * denotes convolution and $w_1(t)$ and $w_2(t)$ denote dynamic weighting functions used for determining controllers K as solutions of the mixed sensitivity problem

$$\left\| \begin{bmatrix} W_1 S \\ W_2 KS \end{bmatrix} \right\|_\infty \leq \gamma$$

$S := (I + GK)^{-1}$ denoting the sensitivity function and $\|\bullet\|_\infty$ representing the H_∞ norm of the system $(\cdot)$ (for more details see [4]), and W_1 and W_2 are appropriate dynamic weighing functions.

A typical Unfalsified Adaptive Control Scheme is presented in Fig. 2, while Fig. 3 presents the algorithm by which controllers are chosen.

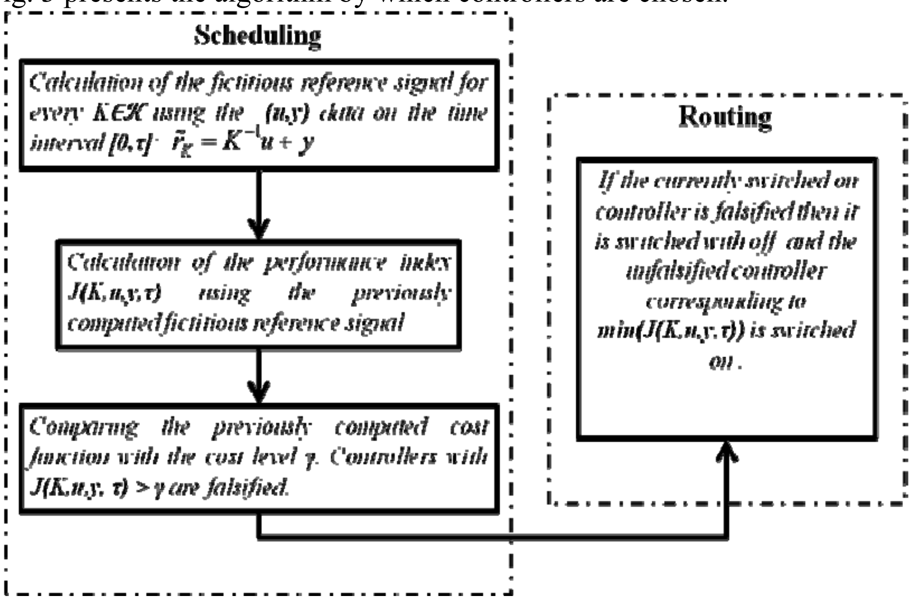

Fig. 3 Falsification algorithm

Unlike previous papers in this paper we will use a simple adaptive switching PID controller based on the one presented in [10]. The PID controller offers the advantage that it is always invertible while the main disadvantage of a lower robustness is partially compensated by being used in an adaptive technique.

3. The bumpless transfer algorithm

The main disadvantage of switching algorithms in general and of unfalsified switching control as presented above, is that, at the moment when a new controller is switched on the control variable jumps to values higher than the actuators of the aircraft can achieve. This is because the new controller has a different transfer function compared to the old controller and thus, when using the same entry signal, it generates a completely different output.

One method to mitigate this is to set the states of the controller so that its output is close to the one of the previous controller.

Thus we impose two simple smoothness conditions on the control variable:

1) **Continuity of the control variable;** the control variable after switching must be the same as it would have been had the switching not occurred
2) **Continuity of the derivative of the control variable;** the derivative of the control variable must remain the same after switching as before switching

In the case of a continuous-time controller we start with the following state space representation of the controller:

$$\begin{aligned} \dot{x}_c &= A_c x_c + B_c e \\ u &= C_c x_c + D_c e \end{aligned} \tag{3}$$

the subscript "*c*" indicates the model of the controller.

Where x_c represents the states of the controller, u the output of the controller, the control variable, e the input of the controller, the tracked signal which is the difference between the reference and the measured output of the plant.

The conditions from above translate in the following equations:

$$\begin{aligned} u_1 &= C_{c2} x_{c2} + D_{c2} e \\ \dot{u}_1 &= C_{c2} \dot{x}_{c2} + D_{c2} \dot{e} \end{aligned} \tag{4}$$

where u_1 represents the last output of the switched off controller and the subscript „2" indicates the states and state-space representation of the new controller to be switched on. The second equation from (4) can be further expanded if we take into account the expression for the derivative of the state vector:

$$\dot{u}_1 = C_{c2}(A_{c2} x_{c2} + B_{c2} e) + D_{c2} \dot{e} \, .$$

Thus we have the following matrix equation system:

$$\begin{aligned} u_1 &= C_{c2} x_{c2} + D_{c2} e \\ \dot{u}_1 &= C_{c2} A_{c2} x_{c2} + (C_{c2} B_{c2} + D_{c2}) \dot{e} \end{aligned}$$

which can be further expanded into

$$\begin{bmatrix} u_{1;1} \\ \vdots \\ u_{1;m} \end{bmatrix} = \begin{bmatrix} c_{c2;11} & \cdots & c_{c2;1n} \\ \vdots & \ddots & \vdots \\ c_{c2;m1} & \cdots & c_{c2;mn} \end{bmatrix} \begin{bmatrix} x_{c2;1} \\ \vdots \\ x_{c2;n} \end{bmatrix} + \begin{bmatrix} d_{c2;11} & \cdots & d_{c2;1p} \\ \vdots & \ddots & \vdots \\ d_{c2;m1} & \cdots & d_{c2;mp} \end{bmatrix} \begin{bmatrix} e_1 \\ \vdots \\ e_p \end{bmatrix}$$

$$\begin{bmatrix} \dot{u}_{1;1} \\ \vdots \\ \dot{u}_{1;m} \end{bmatrix} = \begin{bmatrix} c_{c2;11} & \cdots & c_{c2;1n} \\ \vdots & \ddots & \vdots \\ c_{c2;m1} & \cdots & c_{c2;mn} \end{bmatrix} \begin{bmatrix} a_{c2;11} & \cdots & a_{c2;1n} \\ \vdots & \ddots & \vdots \\ a_{c2;n1} & \cdots & a_{c2;nn} \end{bmatrix} \begin{bmatrix} x_{c2;1} \\ \vdots \\ x_{c2;n} \end{bmatrix} +$$

$$\left(\begin{bmatrix} c_{c2;11} & \cdots & c_{c2;1n} \\ \vdots & \ddots & \vdots \\ c_{c2;m1} & \cdots & c_{c2;mn} \end{bmatrix} \begin{bmatrix} b_{c2;11} & \cdots & b_{c2;1p} \\ \vdots & \ddots & \vdots \\ b_{c2;n1} & \cdots & b_{c2;np} \end{bmatrix} + \begin{bmatrix} d_{c2;11} & \cdots & d_{c2;1p} \\ \vdots & \ddots & \vdots \\ d_{c2;m1} & \cdots & d_{c2;mp} \end{bmatrix} \right) \begin{bmatrix} \dot{e}_1 \\ \vdots \\ \dot{e}_p \end{bmatrix}$$

where m is the number of outputs of the controller, that is the number of control inputs for the plant, n is the number of states of the controller and p is the number of references to be tracked.

The above system of equations can be rewritten as

$$\begin{gathered} c_{c2;11}x_{c2;1} + \ldots + c_{c2;1n}x_{c2;n} = u_{1;1} - d_{c2;11}e_1 - \ldots - d_{c2;1p}e_p \\ \vdots \\ c_{c2;m1}x_{c2;1} + \ldots + c_{c2;mn}x_{c2;n} = u_{1;m} - d_{c2;m1}e_1 - \ldots - d_{c2;mp}e_p \\ \left(c_{c2;11}a_{c2;11} + \ldots + c_{c2;1n}a_{c2;n1}\right)x_{c2;1} + \cdots + \left(c_{c2;11}a_{c2;1n} + \ldots + c_{c2;1n}a_{c2;nn}\right)x_{c2;n} = \\ = \dot{u}_{1;1} - \left(c_{c2;11}b_{c2;11} + \ldots + c_{c2;1n}b_{c2;n1} + d_{c2;11}\right)\dot{e}_1 - \ldots - \left(c_{c2;11}b_{c2;1p} + \ldots + c_{c2;1n}b_{c2;np} + d_{c2;1p}\right)\dot{e}_p \\ \vdots \\ \left(c_{c2;m1}a_{c2;11} + \ldots + c_{c2;mn}a_{c2;n1}\right)x_{c2;1} + \cdots + \left(c_{c2;m1}a_{c2;1n} + \ldots + c_{c2;mn}a_{c2;nn}\right)x_{c2;n} = \\ = \dot{u}_{1;m} - \left(c_{c2;m1}b_{c2;11} + \ldots + c_{c2;mn}b_{c2;n1} + d_{c2;m1}\right)\dot{e}_1 - \ldots - \left(c_{c2;m1}b_{c2;1p} + \ldots + c_{c2;mn}b_{c2;np} + d_{c2;mp}\right)\dot{e}_p \end{gathered} \tag{5}$$

From the system (5) we can determine the new initial condition x_{c2} such that the controller output and its derivative are smooth at the switching moments.

In the case of a discrete-time controller we start from the discrete-time state space representation of the controller:

$$\begin{aligned} x_c((k+1)T_s) &= A_c x_c(kT_s) + B_c e(kT_s) \\ u_c(kT_s) &= C_c x_c(kT_s) + D_c e(kT_s) \end{aligned}$$

where T_s represents the sampling time and k represents the current sample, thus kT_s represents the current time and $(k+1)T_s$ represents the next instant and where the matrices A_c and B_c of the controller are determined by discretization of its continuous-time model.

To represent the derivative of the control variable we will need the derivative of the states of the controller which can be approximated for the current instant as

$$\dot{x}_c\left(\left(k+1\right)T_s\right)=\frac{x_c\left(\left(k+1\right)T_s\right)-x_c(kT_s)}{T_s} \tag{6}$$

obtaining thus equations similar with (5).

Taking into account the case study presented in the next section, the above equations will be detailed for a particular discrete-time SISO controller of second order.

The discrete-time state space representation of such a controller is

$$\begin{bmatrix} x_{c1}\left(\left(k+1\right)T_s\right) \\ x_{c2}\left(\left(k+1\right)T_s\right) \end{bmatrix}=\begin{bmatrix} a_{c11} & a_{c12} \\ a_{c21} & a_{c22} \end{bmatrix}\begin{bmatrix} x_{c1}\left(kT_s\right) \\ x_{c2}\left(kT_s\right) \end{bmatrix}+\begin{bmatrix} b_{c1} \\ b_{c2} \end{bmatrix}e\left(kT_s\right)$$

$$u\left(kT_s\right)=\begin{bmatrix} c_{c1} & c_{c2} \end{bmatrix}\begin{bmatrix} x_{c1}\left(kT_s\right) \\ x_{c2}\left(kT_s\right) \end{bmatrix}+\begin{bmatrix} d_c \end{bmatrix}e\left(kT_s\right).$$

From the second equation above it follows that:

$$u_1\left(kT_s\right)=c_{c2,1}x_{d2,1}\left(kT_s\right)+c_{c2,2}x_{d2,2}\left(kT_s\right)+d_{c2}e\left(kT_s\right)$$

$$\dot{u}_1\left(kT_s\right)=c_{c2,1}\dot{x}_{c2,1}\left(kT_s\right)+c_{c2,2}\dot{x}_{c2,2}\left(kT_s\right)+d_{c2}\dot{e}\left(kT_s\right)$$

where, u_1 represents the last output of the switched off controller and the subscript „c2" indicates the states and state-space representation of the new controller to be switched on. Further based on the approximation (6) one obtains:

$$\dot{u}_1\left(kT_s\right)=c_{c2,1}\frac{x_{c2,1}\left(\left(k+1\right)T_s\right)-x_{c2,1}\left(kT_s\right)}{T_s}+c_{c2,2}\frac{x_{c2,2}\left(\left(k+1\right)T_s\right)-x_{c2,2}\left(kT_s\right)}{T_s}+d_{c2}\dot{e}\left(kT_s\right)$$

$$\begin{cases} u_1\left(kT_s\right)=c_{d2,1}x_{d2,1}\left(kT_s\right)+c_{d2,2}x_{d2,2}\left(kT_s\right)+d_{d2}e\left(kT_s\right) \\ \dot{u}_1\left(kT_s\right)=c_{d2,1}\dfrac{x_{d2,1}\left(\left(k+1\right)T_s\right)-x_{d2,1}\left(kT_s\right)}{T_s}+ \\ \qquad +c_{d2,2}\dfrac{x_{d2,2}\left(\left(k+1\right)T_s\right)-x_{d2,2}\left(kT_s\right)}{T_s}+d_{d2}\dot{e}\left(kT_s\right) \end{cases} \tag{7}$$

$x_{c2,1}\left(\left(k+1\right)T_s\right)$ and $x_{c2,2}\left(\left(k+1\right)T_s\right)$ can be written in relation to $x_{c2,1}\left(kT_s\right)$ and $x_{c2,2}\left(kT_s\right)$, we also simplify the notation by referring from now on to $u_1\left(kT_s\right)$ as *u,* $\dot{u}_1\left(kT_s\right)$ as $\dot{u}$*,* $e\left(kT_s\right)$ and $\dot{e}\left(kT_s\right)$ as e and $\dot{e}$. We will also drop the *c2,* subscript and write $x_{c2,1}\left(kT_s\right)$ and $x_{c2,2}\left(kT_s\right)$ as x_{c1} and x_{c2}. In this way, we rewrite (7)

$$\begin{cases} u = c_1 x_{c1} + c_2 x_{c2} + de \\ \dot{u} = c_1 \dfrac{a_{11}x_{c1} + a_{12}x_{c2} + b_1 e - x_1}{T_s} + c_2 \dfrac{a_{21}x_{c1} + a_{22}x_{c2} + b_2 e - x_{c2}}{T_s} + d\dot{e} \end{cases}$$

from which, by direct computation, one obtains the following values, which the states of the controller must be initialized with:

$$\begin{cases} x_{c1} = \dfrac{u - c_2 x_{c2} - de}{c_1} \\ x_{c2} = \dfrac{c_1\left[\dot{u}T_s - e\left(b_1 c_1 + b_2 c_2\right) - d\dot{e}T_s\right] - \left(u - de\right)\left(c_1 a_{11} + c_2 a_{21} - c_1\right)}{c_1^2 a_{12} - c_2^2 a_{21} + c_2 c_1\left(a_{22} - a_{11}\right)} \end{cases} \tag{8}$$

4. A case study

The following case study was carried out using the linearized short period dynamics of the ADMIRE aircraft model. We used the methodology presented in Section 2 to have the algorithm switch among different gains of a PID controller and chose the most appropriate for the flight regime.

The ADMIRE model has been trimmed (linearized) at the flight condition characterized by Mach Number 0.75, altitude 5000 and angle of attack 12 degrees.

The reference signal "*r*" is the desired angle of attack of the aircraft and the control variable "*u*" is the elevon position. The candidate controller set is build similar to [10] but instead of the derivative part being implemented in the feedback it is implemented as feed-forward. The general form of the PID controller can be seen in Fig. 3.

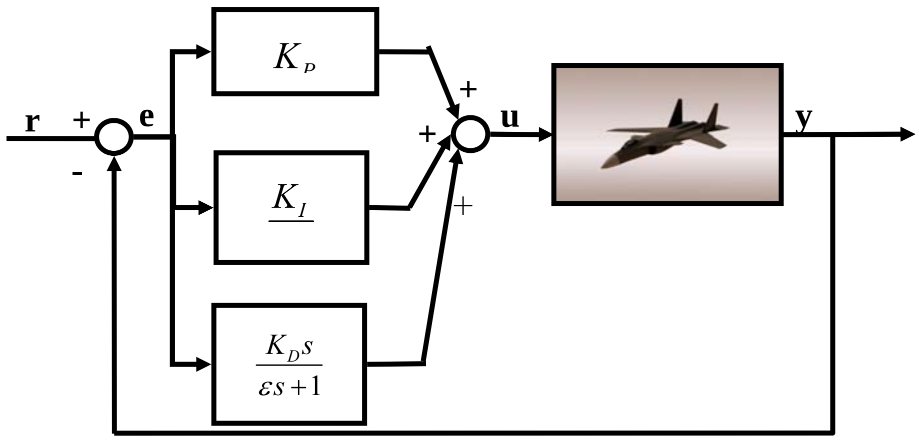

Fig. 4 PID controller arrangement

There K_P represents the proportional gain, K_I the integrative gain and K_D the derivative gain. The transfer function of the controller is of the following form:

$$\frac{u(s)}{e(s)}=\frac{s^2\left(K_D+K_P\varepsilon\right)+s\left(\varepsilon K_I+K_P\right)+K_I}{\varepsilon s^2+s} \tag{9}$$

where u is the output of the controller, the control variable, e is the tracking error and ε is a number fixed a 0.01.

The gains of the candidate controllers belong to the following sets:

- $K_P \in \{5,10,15,20,25\}$
- $K_I \in \{0.5,1,5,10,25\}$
- $K_D \in \{0.6,0.5\}$

This yields a total of 100 candidate controllers.

The candidate controllers where discretized in Matlab using the c2d.m function and appropriate state space representations where generated for each of their inverses. The virtual reference for each one of them was thus computed by applying as input to the state space realization of the inverse, the control variable generated by the on-line controller.

As performance index we used one similar to the one given in [10]. We impose the following condition to the candidate controllers:

$$\left\|\omega_1 *\left(rv_i-y\right)\right\|_t^2+\left\|\omega_2 * u\right\|_t^2 \leq \left\|rv_i\right\|_t^2 \tag{10}$$

where rv_i is the virtual reference corresponding to the “i”-th controller, y is the measured output, u is the control variable * denotes convolution and thus the products $\omega_1 * (r_v - y)$ and $\omega_2 * u$ are the signals through the weighing filters $W_1(s) = \frac{10s+1}{s+0.1}, W_2(s) = \frac{0.1s+0.1}{0.01s+1}$ when $r_v - y$, respectively u are given as inputs to the two filters.

In (10), $\|f\|_t^2 = \int_0^t |f(t)|^2 \, dt$ thus one obtains the following performance index:

$$J = \int_0^t \left(\left| \omega_1 * \left(rv_i(t) - y(t) \right) \right|^2 + \left| \omega_2 * u(t) \right|^2 - \left| rv_i(t) \right|^2 \right) dt$$

Considering that the switching algorithm requires a discrete-time implementation of the controllers the performance index can be further written for a discrete-time case as:

$$J(i, kT_s) = J(i, (k-1)T_s) + \int_{(k-1)T_s}^{kT_s} \left(\left| \omega_1 * \left(rv_i(t) - y(t) \right) \right|^2 + \left| \omega_2 * u(t) \right|^2 - \left| rv_i(t) \right|^2 \right) dt \quad (11)$$

By approximating the integral in (11) as the area under the graph we obtain the following expression which we implement in our case study:

$$\begin{aligned} J(i, kT_s) = J(i, (k-1)T_s) + \frac{1}{2} T_s \Bigg\{ \Bigg[\left| \omega_1 * \left(rv_i(kT_s) - y(kT_s) \right) \right|^2 + \\ + \left| \omega_2 * u(kT_s) \right|^2 - \left| rv_i(kT_s) \right|^2 \Bigg] + \Bigg[\left| \omega_1 * \left(rv_i((k-1)T_s) - y((k-1)T_s) \right) \right|^2 + \\ + \left| \omega_2 * u((k-1)T_s) \right|^2 - \left| rv_i((k-1)T_s) \right|^2 \Bigg] \Bigg\} \end{aligned} \quad (12)$$

The used algorithm is the one presented in Fig. 3 with the exception that after switching the new controller is initialized with the states from equation (8) to achieve a bumpless transfer. Also, the switching algorithm is not run at each sample time. A “dwell time” was introduced as the requirement to use the derivative of several measurements as inputs in the algorithm for bumpless transfer means that several sample time intervals have to pass for an accurate measurement to be obtained. Several dwell times were tried, and the dwell time of 0.08 seconds was chosen as the most representative for the case study.

The set of candidate controllers was random by chosen without a previous tuning of the PID controllers so the output of the plant is not optimum. Also, the initial controller was not stabilizing the dynamics used in the simulation. The results of the case study are presented in Figs. 5 through 10.

They show that the algorithm for bumpless transfer helps at the moment of switching. The initial spike present in the first two figures which show the control variable is generated by the fact that zero initial conditions were used for the states of the controller. When the algorithm for bumpless transfer was turned off there were also big spikes at the moments of switching in the region of 10-20 degrees. Also, the switching algorithm converged very slowly to a final controller. On the other hand when the algorithm for bumpless transfer is turned on the spikes at the moments of switching are much smaller and also the amplitude of the oscillation of the control variable is halved. The algorithm for bumpless transfer also has an effect on the plant output: the transitory behavior is much better, the overshot is smaller and the angle-of-attack converges to the reference much faster. Also, the variation of the pitch rate (which was not commanded in the study, but which is influenced by the angle-of-attack) is much smoother, with smaller spikes.

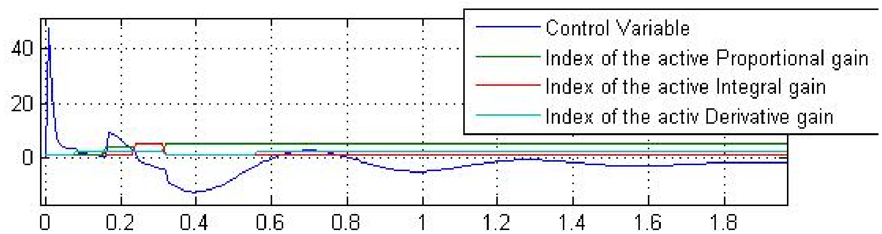

Fig 5 Control variable with the algorithm for bumpless transfer turned off. Dwell time 0.08s.

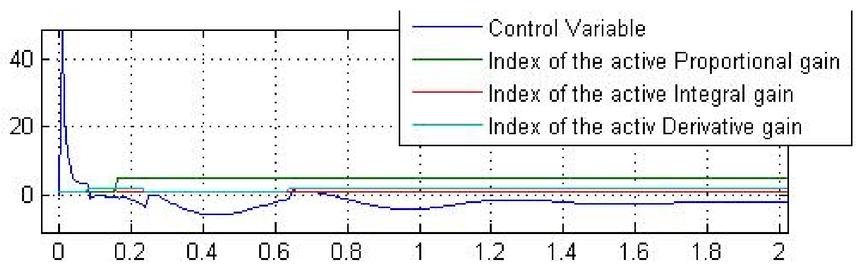

Fig 6 Control variable with the algorithm for bumpless transfer turned on. Dwell time 0.08

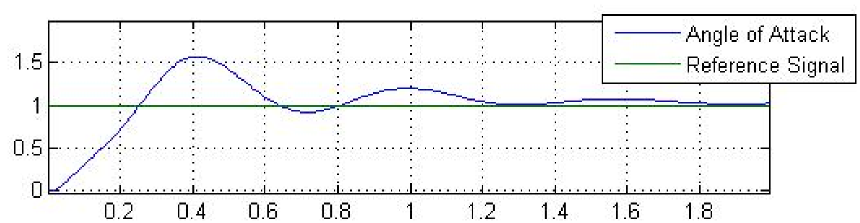

Fig 7 Variation of the angle-of-attack with the algorithm for bumpless transfer turned off. Dwell time 0.08s.

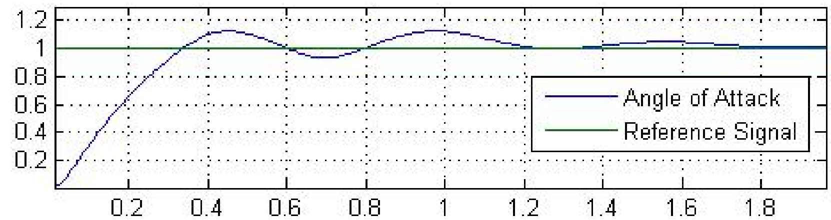

Fig 8 Variation of the angle-of-attack with the algorithm for bumpless transfer turned on. Dwell time 0.08s

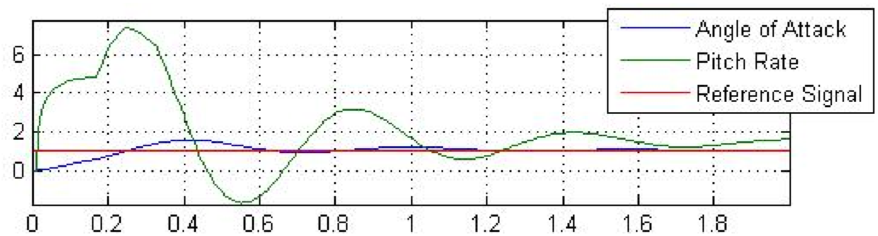

Fig 9 Variation of the angle-of-attack and of the pitch rate with the algorithm for bumpless transfer turned off. The reference signal represents the commanded angle-of-attack. Dwell time 0.08s.

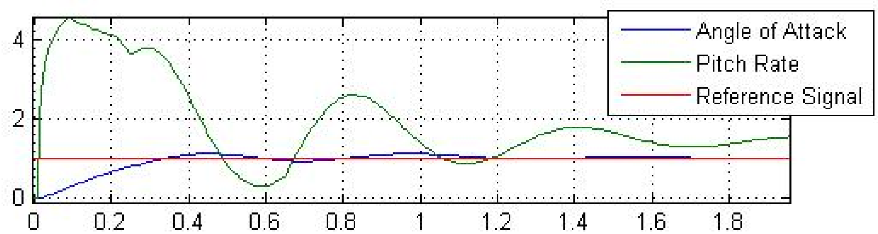

Fig 10 Variation of the angle-of-attack and of the pitch rate with the algorithm for bumpless transfer turned on. The reference signal represents the commanded angle-of-attack. Dwell time 0.08s.

5. Conclusions

The algorithm presented in this paper seems promising. It smoothens the control variable and improves the behavior of the measured output. There are also some issues which will require further research:

- the algorithm showed deteriorating performance as the dwell time was increased, at dwell times close to one second, the switching algorithm seems to be bumpless by itself without further augmentation, future research will have to be conducted as to the choose the optimum dwell time which tunes the algorithm for both rapid adaptation and a smooth behavior of the aircraft.
- Analysis of the performances obtained using other classes of controllers with both the switching algorithm and the bumpless transfer algorithm.

- Investigation of the influence of the sampling period over the performances of the automatic flight control system with switching and bumpless transfer

Acknowledgment
This paper is financed by grant POSDRU 7173 through contract POSDRU/6/1.5/S/19

B I B L I O G R A P H Y

[1] *Baldi, S., Battistelli, G., Mosca, E. & Tesi, P.* Multi-Model Unfalsified Supervisory Switching Control. Automatica 46, pp. 249-259, 2010.
[2] *Dehghani, A., Anderson, B. D. O. & Lanzon,* A. Unfalsified Adaptive Control: A New Controller Implementation and Some Remarks. Kos, Greece, s.n, , July 2-5, 2007.
[3] *Morse, A. S.* Control Using Logic Based Switching. In: Trends in Control A European Perspective. s.l.:Springer-Verlag, , 1995, pp. 69-113.
[4] *Safonov, M. G. & Tsao, T. C.* The Unfalsified Control Concept and Learning. IEEE Transactions on Automatic Control, AC-42(6), June 1997, pp. 842-847.
[5] *Hanus, R., Kinnaert, M. & Henrotte, J. -L.*. Conditioning technique, a general anti-windup and bumpless transfer method. Automatica, 23(6), 1987, pp. 729-739.
[6] *Arehart, A. B. & Wolovich, W. A*. Bumpless switching controllers. s.l., IEEE Conference on Decision and Control, , December 1996, pp. 1654-1655.
[7] *Cheong, S.-Y. & Safonov, M. G.* Bumpless Transfer for Adaptive Switching. Seoul, COEX, Korea, South, 17th IFAC World Congress, 2008.
[8] *Neamtu, A. S. & Stoica, A. M.*, Adaptive robust design of unmanned combat air vehicle automatic control system, 27th international congress of the aeronautical sciences, Nice, France, 2010.
[9] *Neamtu, A. S. & Stoica, A. M.*, A comparison of Adaptive Supervisory Switching Control Schemes For High Maneuverability Aircrafts. 18th International Conference on Control Systems and Computer Science, Bucharest, Romania, May, 2011.
[10] *Jun, M. & Safonov, M.*, Automatic PID tuning: An Aplication of Unfalsified Control, IEEE International Symposium on Computer Aided Control System Design, Kohala Coast, Island of Hawai'i, Hawaii USA, august 22-27 1999.